Theory and Experimental Results of a New Diamond Surface-Emission Cathode

Michael W. Geis, Nikolay N. Efremow, Jr., Keith E. Krohn, Jonathan C. Twichell, Theodore M. Lyszczarz, Rafael Kalish, James A. Greer, and Martin D. Tabat

■ A new electron-emission mechanism combines the enhanced electric field of a triple junction at the intersection of metal and diamond interfaces in vacuum with the negative electron affinity (NEA) of the diamond surface. This new surface-emission mechanism is compared to two common cathode mechanisms—geometric electric-field enhancement and Schottky-diode electric-field enhancement with an NEA semiconductor. Unlike these two mechanisms, in which electrons tunnel from metal into vacuum or into the conduction band of an NEA semiconductor, in our mechanism electrons tunnel from metal into surface states at the interface of an NEA semiconductor and a vacuum. Once in these states, the electrons are accelerated to sufficient energies to be emitted from the surface into vacuum.

New cathodes designed to maximize the surface-emission mechanism exhibit improved consistency and reduced operating voltage when compared to cathodes that use other mechanisms. Gated surface-emission cathodes emit measurable current densities greater than 10^{-6} A m^{-2} at gate voltages of 3 to 4 V, and current densities greater than 10 A m^{-2} at 6 to 10 V (which are useful for flat-panel displays). Depending upon the fabrication method, these cathodes can emit beams of nearly monoenergetic electrons with energy almost equal to the gate voltage, which varies from approximately 0 to 6000 eV. Some of these devices exhibit excessive gate currents that can vary from 0.2 to 10^5 times the emitted current, which may limit potential applications for the devices.

DIAMOND SURFACE-EMISSION cathodes show great promise for use in flat-panel displays, fluorescent lighting, and power vacuum tubes that switch thousands of amperes. Unlike metal-emission cathodes, diamond surface-emission cathodes can operate at low voltages and would be easy and inexpensive to fabricate. Although many research groups have reported emission from diamond and amorphous diamond-like films at electric fields on the order of a megavolt per meter, the use of these materials as cathodes is limited by their unreliable performance [1, 2]. Researchers generally attribute the unreliable performance to inconsistent bulk properties of the diamond cathode material, which is believed to cause electron emission from only a small number of spatially localized sites.

We have found a surface-emission mechanism that may help explain nonuniform emission in diamond: enhanced electron emission at the triple-junction interface of a diamond surface, a conductive region, and a vacuum. Our research suggests that a discontinuous diamond film with an abundance of these interfaces could be a better electron emitter than the conventional approach of a continuous diamond film.

In this article, we compare our surface-emission mechanism with two common field-emission mechanisms—geometric electric-field enhancement and Schottky-diode electric-field enhancement with a negative electron affinity (NEA) semiconductor [2]. In an NEA semiconductor, by definition, the minimum energy of electrons in the conduction band is greater than the minimum energy of electrons in a vacuum. The surface-emission mechanism combines the high electric fields that can be obtained at a triple junction [3, 4] with the high-mobility surface states known to form on NEA-semiconductor surfaces [5]. The surface-emission mechanism explains many observed diamond-cathode emission properties, and has brought about changes in diamond-cathode design and fabrication, resulting in considerable improvement in performance. Gated cathodes fabricated to maximize the triple-junction NEA-surface-emission mechanism, referred to as surface-emission cathodes, emit measurable current densities equal to and above 10^{-6} A m^{-2} at gate voltages of 3 to 4 V, and useful current densities greater than 10 A m^{-2} at 6 to 10 V. In some cases, as shown later in the article, these electrons are emitted as a collimated beam of nearly monoenergetic electrons. With our present designs, some surface-emission cathodes suffer from excessive gate current in the range of 0.2 to 10^5 times the emitted current, which limits their potential applications.

Three Electron-Emission Mechanisms

The most commonly used field-emission mechanism, illustrated in Figure 1, is geometric electric-field enhancement. This technique applies an electric field to a sharpened conductive cone with a high aspect ratio of height to base diameter. According to theory, no measurable emission occurs from a perfectly smooth metal surface at fields less than 10^9 V m^{-1}. But emission occurs with the sharpened conductive cone at average applied fields of 10^7 to 10^8 V m^{-1}.

The emission-current density J (in A m^{-2}) is related to the local electric field E (in V m^{-1}) at the emitting surface by the Fowler-Nordheim equation,

$$J = \frac{eE^2}{8\pi h\Phi} \exp\left[\frac{-4}{3} \sqrt{\frac{8\pi^2 m}{h^2}} \Phi^{3/2} \frac{V(E,\Phi)}{(e^{3/2}E)}\right], \quad (1)$$

where Φ is the work function of the cone material in eV, e is the charge of an electron (1.602×10^{-19} C), h is Planck's constant (4.136×10^{-15} eV-sec), m is the mass of an electron (9.109×10^{-31} kg), and $V(E, \Phi)$ is Nordheim's elliptic function [6]. The elliptic function allows for barrier lowering by the image charge of the tunneling electron in the metal cone, and varies from zero to one. Accurate current-density calculations using Equation 1 are nearly impossible, however, because the local geometrically enhanced electric field at the emitting surface is difficult to determine and the work function Φ can vary significantly over an atomic scale. Consequently, researchers approximate the current density J with the equation

$$J \cong E_{\text{avg}}^2\, a \exp\left(\frac{-b}{E_{\text{avg}}}\right), \quad (2)$$

where a and b are variables that can be adjusted to fit the experimental data and are used to characterize cathode performance.

Geometric electric-field enhancement explains why the electric field required to produce an emission current is lower for burnished stainless steel than for polished stainless steel. The polished surface emits measurable currents greater than 10^{-10} A to a 1-mm-diameter anode spaced 100 μm away at an applied field of 10^8 V m^{-1}. When the surface is burnished with 600-grit emery cloth to create thousands of tiny cones, the same currents are obtained at an applied field of 10^7 V m^{-1}. For practical applications, arrays of cathodes consisting of metal cones and a metal grid structure spaced 100 nm to 10 μm apart [7, 8] require 20 to 200 V between the cones and the grid to obtain average current densities greater than 10 A m^{-2}.

Figure 2 illustrates the second electron-emission mechanism, known as Schottky-diode electric-field enhancement. This mechanism requires a semiconductor that is doped with an electron donor impurity and has an NEA-semiconductor surface-vacuum interface. The semiconductor forms a Schottky diode with the metal substrate. The magnitude of the emitted current is limited by electrons tunneling through the metal-semiconductor Schottky diode and not by electron emission from the semiconductor into vacuum. When an electric field is applied across the
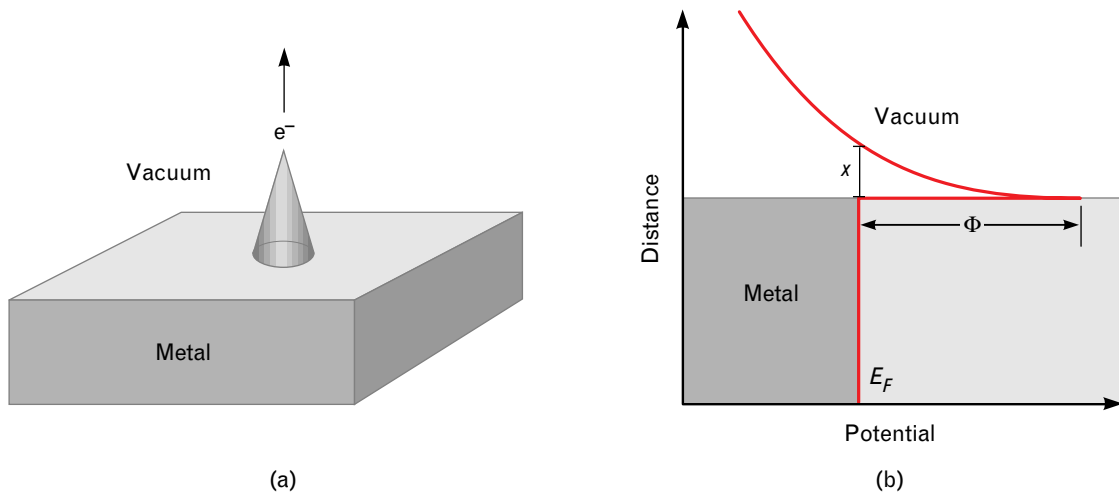
FIGURE 1. Geometric electric-field enhancement at the top of a sharpened conductive cone. (a) An electric field applied to a sharpened conductive cone produces electron emission at the top of the cone. This emission occurs at average electric-field values that are lower than those needed for emission from a smooth metal surface. (b) The plot of potential energy as a function of distance from the cone tip into vacuum, where E_F is the Fermi energy in the metal, illustrates the magnitude of the potential-energy barrier Φ at the metal-vacuum interface. To be emitted from the conductive cone, electrons must tunnel a distance x through the potential barrier.

semiconductor, the dopants become positively ionized and form a depletion region at the metal-semiconductor junction. If diamond is used as the semiconductor, the electric field at this junction is often greater than $10^9 \mathrm{~V~m^{-1}}$, causing the electrons to tunnel from the metal into the semiconductor. Electrons in the semiconductor can be easily injected into the vacuum. Geometric electric-field enhancement created by roughening the metal-semiconductor interface can boost electron emission further.
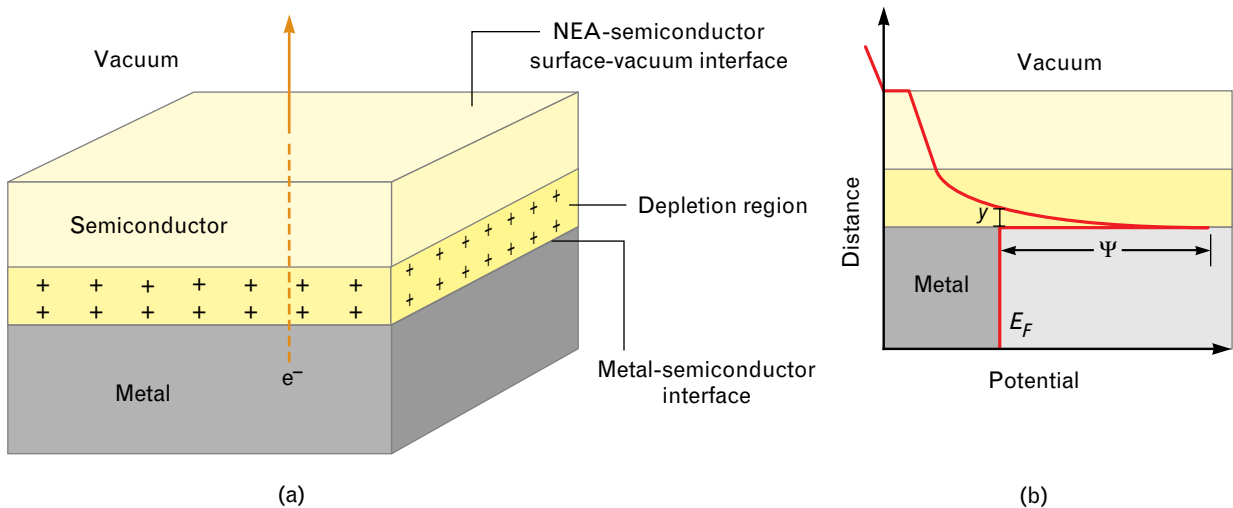
FIGURE 2. Cross section of metal-semiconductor and NEA-semiconductor surface-vacuum interfaces for Schottky-diode electric-field enhancement with a semiconductor doped with an electron donor impurity. (a) When an electric field is applied across the semiconductor, the dopants become positively ionized and form a depletion region at the metal-semiconductor interface. Electrons tunnel from the metal into the semiconductor, and are emitted at the NEA-semiconductor surface-vacuum interface. (b) The plot of potential energy as a function of distance, where E_F is the Fermi energy in the metal, illustrates the potential-energy barrier Ψ at the metal-semiconductor interface. To be emitted from the metal substrate, electrons must tunnel a distance y through the potential barrier.

Schottky-diode electric-field enhancement has been discussed in more detail elsewhere [2], and variations of this mechanism have been used to explain many experimental results [9–12]. The current density J is related to the semiconductor doping density n (in m^{-3}), the potential-energy barrier height Ψ (in eV) at the metal-semiconductor interface, and the potential drop V across the semiconductor by

$$
\begin{aligned}
J &= \frac{en}{\pi h \varepsilon \varepsilon_0} \frac{1}{P^2} \exp\left[-\left(\frac{\pi V}{h}\right)\sqrt{\frac{\varepsilon \varepsilon_0 m_e}{en}} \, T\right] \\
&\approx a_1 V^2 \exp\left[\frac{-b_1}{\sqrt{V}}\right] \text{ for } V >> \Psi ,
\end{aligned}
\tag{3}
$$

where

$$
T = D + \frac{\left(1-D^2\right)}{2}\ln\left[\frac{(1-D)}{(1+D)}\right] \approx \frac{2D^3}{3} + \frac{2D^5}{15} ,
$$

$$
P = -D\ln\left[\frac{(1-D)}{(1+D)}\right] \approx 2D^2 + \frac{2D^4}{3} ,
$$

$$
D^2 = \frac{\Psi}{V} ,
$$

and where ε_0 is the permittivity of vacuum (8.85×10^{-12} F m^{-1}), ε is the dielectric constant of the semiconductor (5.7 for diamond), m_e is the effective mass of the electron in the semiconductor (about 0.3 times the mass of an electron for diamond), and a_1 and b_1 are functions of ε, Ψ, m_e, and n. This equation was derived by using the WKB approximation [13].

The electron emission increases as the doping density n increases and the dielectric constant ε, the effective mass of the electron m_e, and the barrier height Ψ decrease. Although the functional form of Equation 3 is substantially different from Equation 1, both functions will usually describe the data when the measured emitted current density from a cathode is plotted against the voltage required for emission. Thus we cannot easily distinguish between the two mechanisms on the basis of the emission parameters of the cathode. As with Equation 1, accurate emission-current calculations using Equation 3 are almost impossible because not enough of the parameters are known

to sufficient accuracy [14]. Arrays of these cathodes emit current densities above 10 A m^{-2} when potentials of 10 to 20 V are applied between the metal substrate contacting the semiconductor and a metal gate structure spaced about 1 μm away [2, 15].

Figure 3 illustrates the third electron-emission mechanism, known as triple-junction electric-field enhancement, or surface emission. Surface emission combines two physical phenomena—electric-field enhancement at a triple junction [3, 4, 16] and high electron mobility at an NEA-semiconductor surface-vacuum interface [5]. In this mechanism, an impurity-donor-doped NEA semiconductor is used in the triple-junction geometry. When a negative bias on the metal substrate produces an electric field along the semiconductor surface, a substantial positive charge can form on the surface and in the bulk of the semiconductor near the triple junction. Part of this charge comes from the Schottky diode, and is formed by the semiconductor and the metal substrate. If the field is large enough, electrons tunnel from the metal substrate onto the semiconducting surface with sufficient energy to cause secondary electron emission, which further increases positive charge at the surface. Depending upon the angle θ between the semiconductor-vacuum interface and the metal substrate, as shown in Figure 3, the electric-field enhancement can be larger than that obtained with the two mechanisms discussed previously [17].

We use both the electric-field enhancement at a triple junction and the property of high electron mobility on an NEA-semiconductor surface-vacuum interface to explain the electron-emission mechanism. The high electron mobility [5] is the result of surface states in which electrons in vacuum are bound to a surface by their image charge in the material, but are not allowed to pass through the surface because of quantum mechanical considerations. We discuss surface states in more detail in the next section. Emission from surface cathodes occurs when electrons tunnel from the metal substrate through the barrier at the triple junction. The barrier height is difficult to determine but may be as little as 1 eV or as much as the work function of the metal less the binding energy of the surface state. This barrier height for tunneling at the triple junction is less than the corresponding bar-
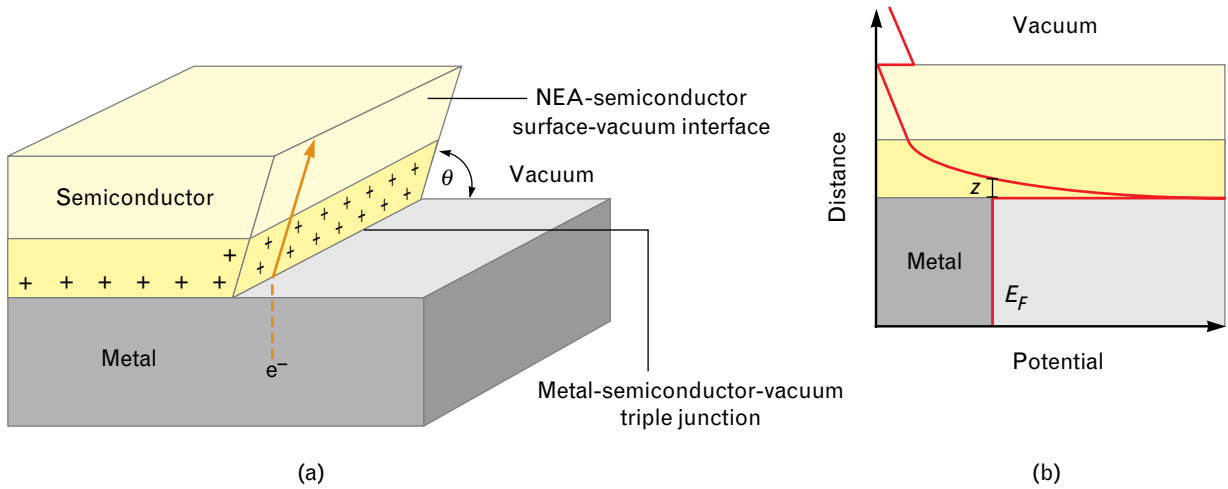
FIGURE 3. Triple junction (metal-semiconductor-vacuum) electric-field enhancement. (a) The combination of an impurity-donor-doped semiconductor and the high mobility of electrons at the NEA-semiconductor surface-vacuum interface causes electrons to tunnel from the metal substrate onto the surface of the semiconductor. Depending on the angle θ, the electric-field enhancement can be larger than that obtained with the two mechanisms illustrated in Figures 1 and 2. (b) The plot of potential energy along the semiconductor-vacuum interface, where E_F is the Fermi energy in the metal, illustrates the potential-energy barrier. To be emitted at the semiconductor-vacuum interface, electrons must tunnel a distance z from the metal substrate into the triple-junction region. This potential barrier, while difficult to determine, is known to be less than the potential barrier for the geometric electric-field enhancement mechanism.

rier height for geometric electric-field enhancement. A potential of only 6 to 10 V is all that need be applied across an emitting-surface length of 1.5 μm to obtain currents equivalent to 10 A m^{-2}.

Surface States on NEA Semiconductors

Surface states on NEA semiconductors come from the semiconductor-vacuum interface. They differ from the interface states associated with silicon dioxide on silicon, for example, in which an electron can be confined by an atom or a broken bond. With NEA materials, electrons in a vacuum are attracted to both dielectrics and metals by their effective image charge in the material. These electrons do not have enough energy to pass into the semiconductor's conduction band from the vacuum. Instead the electron resides in electrostatic surface states, 0.1 to 10 nm above the surface.

Surface states on NEA semiconductors have been studied since the 1970s [5, 18]. Most of this research was performed with liquid He^4, an NEA material, with the conduction band approximately 1 eV above the vacuum level. Other materials, such as liquid He^3 and liquid neon, have demonstrated similar effects,

and recent room-temperature results were reported on metals [19] and insulators [20].

Figure 4 shows the potential energy produced by the effective image charge for liquid He^4 and diamond. The resulting one-dimensional hydrogenic surface states have binding energies E in eV, which are approximated by

$$E \approx R \frac{(\varepsilon - 1)^2}{\left[4n(\varepsilon + 1) \right]^2},\qquad (4)$$

where R is the Rydberg constant (13.7 eV), n is the quantum number, and ε is the dielectric constant of the NEA semiconductor (1.057 for liquid He^4 and 5.7 for diamond). The average distance d that an electron in the lowest energy state is displaced from the interface is given by

$$d \approx 4a_0 \frac{(\varepsilon + 1)}{(\varepsilon - 1)},\qquad (5)$$

where a_0 is the Bohr radius (0.0529 nm). For a liquid-He^4 interface, the binding energy was measured to be 0.7 meV below the vacuum level, with the electron
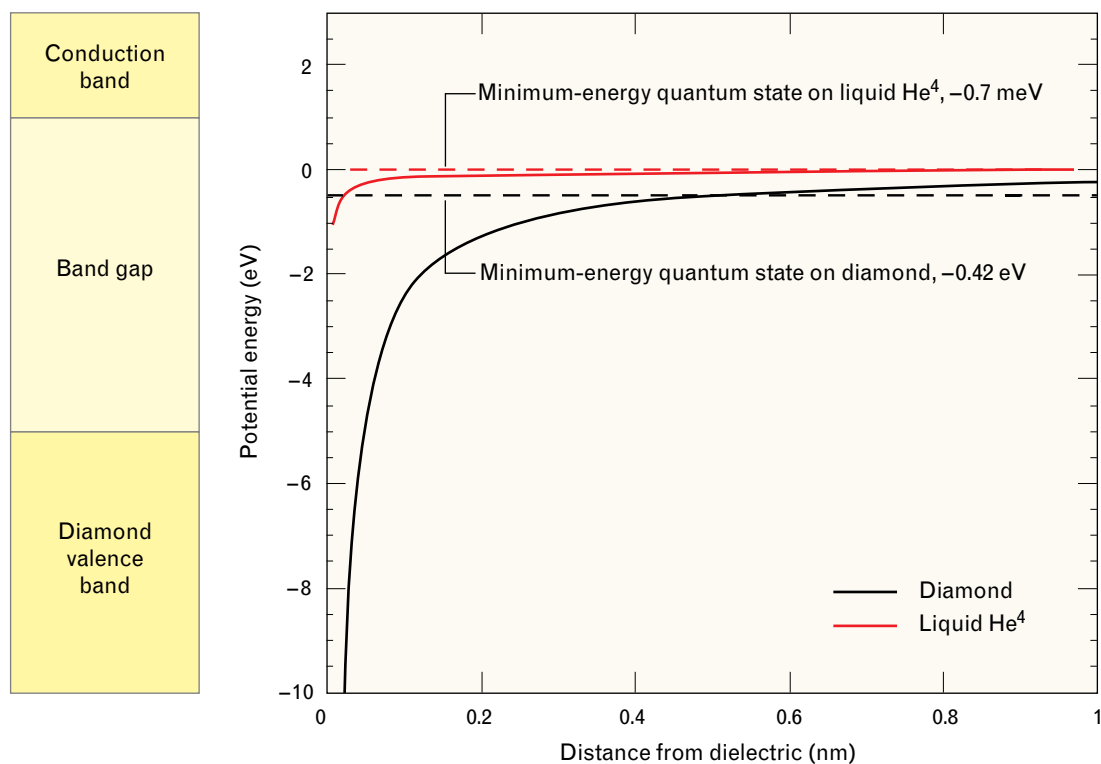
FIGURE 4. Potential-energy curves as a function of distance from the liquid-He^4–vacuum and diamond-vacuum interfaces. These curves show the minimum-energy quantum states for an electron on liquid-He^4 and diamond surfaces. The bar on the left shows the approximate energy positions of the conduction bands for liquid He^4 and diamond, and the valence band for diamond.

about 7.5 nm above the surface [21]. Diamond has a calculated minimum surface-state energy 0.42 eV below the vacuum level, with the electron about 0.3 nm above the surface.

Experiments

A variety of experimental results led us to consider NEA-semiconductor surface emission for electron emission from diamond. Figure 5 depicts a type-Ib cubo-octohedron diamond, about 3 mm across, containing a deep donor of substitutional nitrogen. The diamond has been implanted with 34 keV lithium ions at 200°C to a dose of 4×10^{16} cm^{-2} to enhance the electrical contact between the metal support and the diamond [22, 23]. The anode, which can be moved from a point touching the diamond to several centimeters above the diamond, was at first a molybdenum rod 0.5 mm in diameter. In later experiments we used a square phosphor screen approximately one centimeter on a side. The diamond was prepared for emission by exposing it to an oxygen discharge, coating it with cesium, and reexposing it to oxygen, a surface procedure known to enhance diamond's NEA property [24, 25]. Next, the molybdenum anode was positively biased to obtain stable electron emission from the diamond. During emission, a greenish-yellow fluorescence originated from the ion-implanted region and progressed up the side of the diamond, around the top edge, and across the top surface. We believe the fluorescence originated from electrons traveling across the diamond surface rather than through its bulk. The path of the electrons depended on the surface irregularities of the diamond. Once on the top surface, the electrons jumped the 0.0-to-0.8-mm gap between the top diamond surface and the positively charged movable anode.

When the molybdenum anode was moved from a point touching the diamond to a point 0.5 mm above the diamond, the anode voltage had to be increased from 7 to 8 kV to maintain a constant emission cur-

rent of 10^{-5} A. This increase indicates that most of the potential drop, about 7 kV, appears across the diamond and is not being expended in the vacuum gap between the diamond and the anode [25]. When a square phosphor screen was used as an anode and placed on the diamond surface, the screen fluoresced where it met the diamond, as shown in Figure 5(b). The phosphor screen fluoresced only when hit with electrons of energy greater than 1 keV, implying that these electrons have considerable energy while still on the diamond surface.

From our experiments with both of these anodes, we theorize that these electrons are field emitted from the implanted region into semiconductor-vacuum surface states. Once in these surface states, the electrons can be accelerated to energies above 1 keV. Electrons with similar energies appear to be emitted after traveling through the bulk of diamond and other semiconductors [26, 27], but often we cannot distinguish electrons that move across the surface from those which are conducted through the bulk of the semiconductor.

To characterize the emission further, we coated a type-Ib diamond 100-μm plate with electron-beam-evaporated nickel on the back side and graphite on top to form a conductive layer. The graphite layer was formed by sputtering the diamond surface with 1200-eV xenon ions. The diamond was then cleaved to obtain a clean, undamaged surface, as illustrated in Figure 6. When a potential of a few kilovolts was placed between the nickel and the graphitized layer, electrons were emitted into vacuum. This emission was further increased with the same oxygen-cesium treatment previously described [26], but no oxygen discharge was used because that would remove the graphite layer. Figure 7 shows typical currents obtained from these surface-emission cathodes. By using a movable phosphor screen, we determined that the electrons originated from the cleaved surface with nearly the same energies, i.e., within 50 eV of the applied potential. Because we wanted to measure the energies of the electrons, we modified the experiment to include an energy analyzer, as shown in Figure 8.

The mechanism used to explain the surface emission relies upon positive charges at or near the diamond surface to create a large electric field at the triple junction. From previous experiments we know that nitrogen impurities in diamond can be positively ionized and remain charged for days, but once the diamond is exposed to room light, photogenerated electrons in the diamond will neutralize the nitrogen impurities. Figure 9 shows the effect of 100 W m^{-2} of
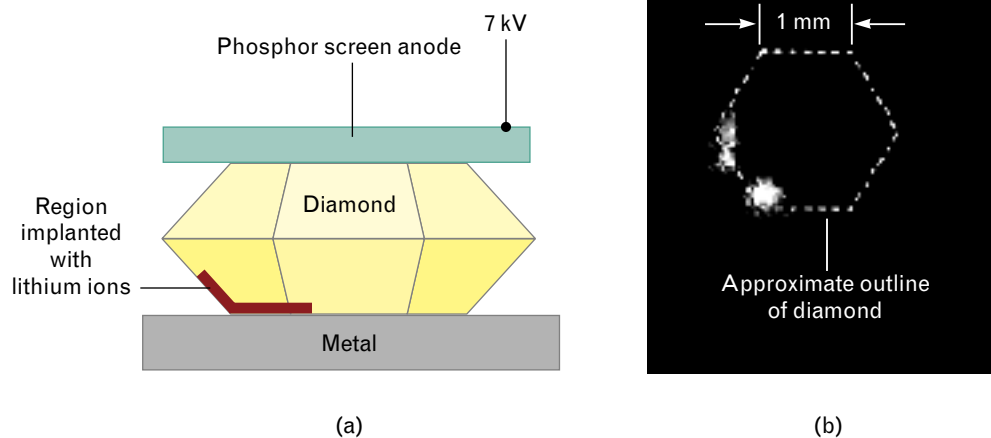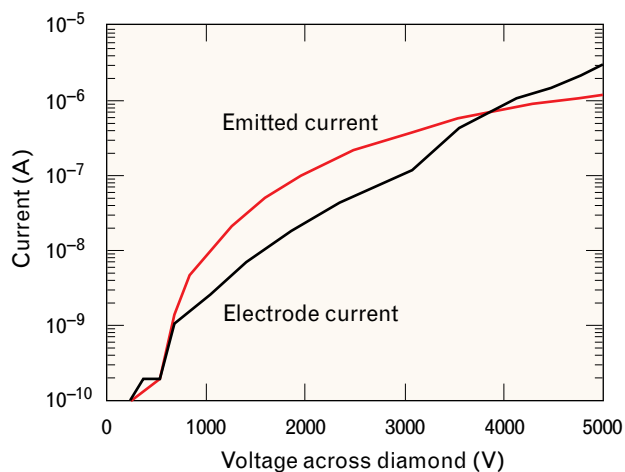

FIGURE 5. (a) Diagram of lithium-ion-implanted diamond with a phosphor screen anode placed on top of the diamond. (b) Observed fluorescence of the phosphor screen is directly under the portion of diamond implanted with lithium. The phosphor screen continued to fluoresce when lifted several hundred microns above the diamond, but the regions of fluorescence moved away from the edge of the diamond to the center of the diamond and became more diffuse.
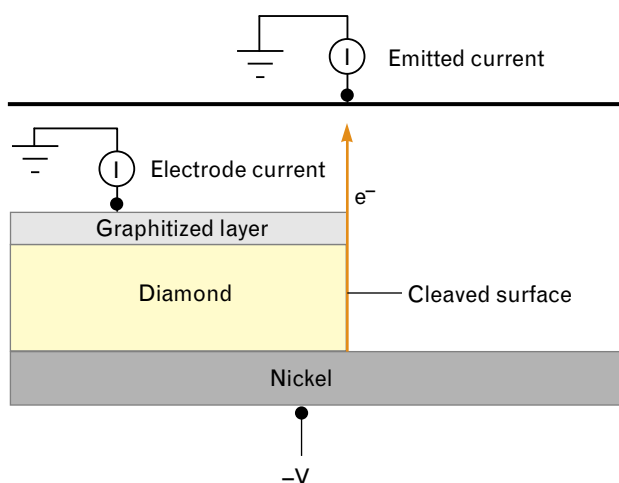
FIGURE 6. Surface-emission cathode experiment using the cleaved surface of diamond to emit electrons. Electrons tunnel from the nickel metal substrate onto the diamond surface from which they are emitted into a vacuum.

FIGURE 7. Plot of emitted and electrode currents as a function of applied voltage for the surface-emission cathode shown in Figure 6. As the voltage across the diamond increases, both currents increase.

incandescent illumination on the diamond, where the emitted current is larger in the dark than with the illumination on. In the dark, measurable emission occurs for potentials as low as 150 V across the diamond. With the illumination on, the emission decreases and is not measurable until a potential greater

than 1 kV is applied. If the cathode is first illuminated with no applied potential, and then the illumination is turned off and potentials from 0 to 5 kV (in increasing order) are applied to the diamond, the emission at the start of the experiment nearly matches the emission measured in the light (blue curve). After
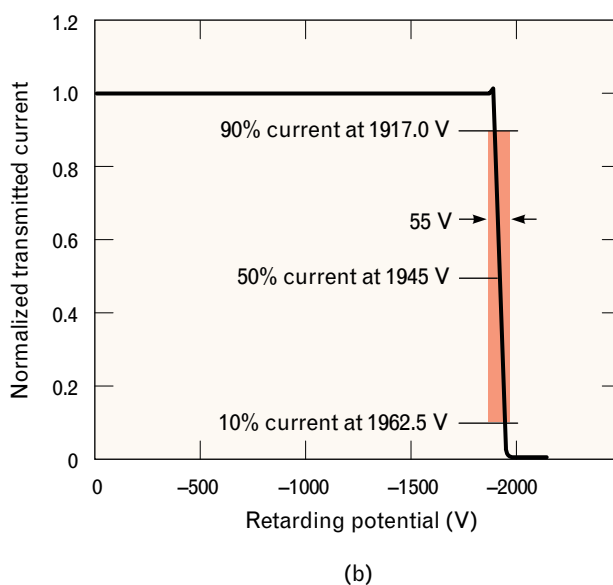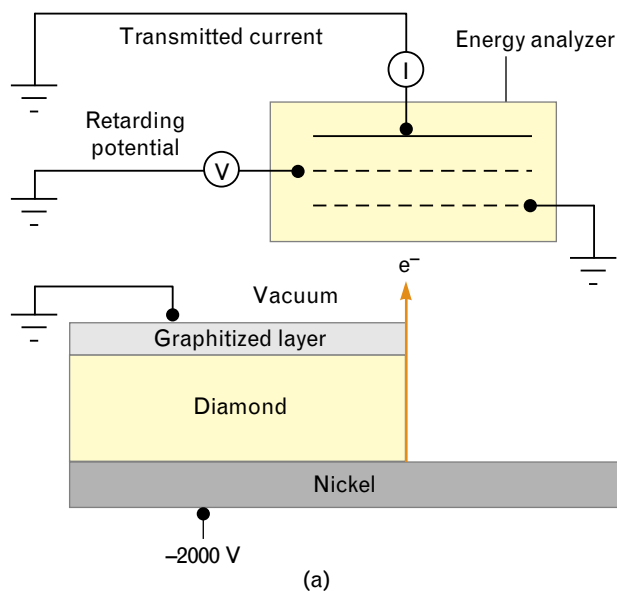
FIGURE 8. (a) Diagram of a retarding energy analyzer used to estimate the electron's energy. Electrons with an absolute energy value less than the retarding potential do not contribute to the transmitted current. (b) Transmitted current as a function of retarding potential. The red band in the figure highlights the results of the experiment. Up to 90% of the electrons have energies greater than 1917.0 eV, and fewer than 10% of the electrons have energies greater than 1962.5 eV.
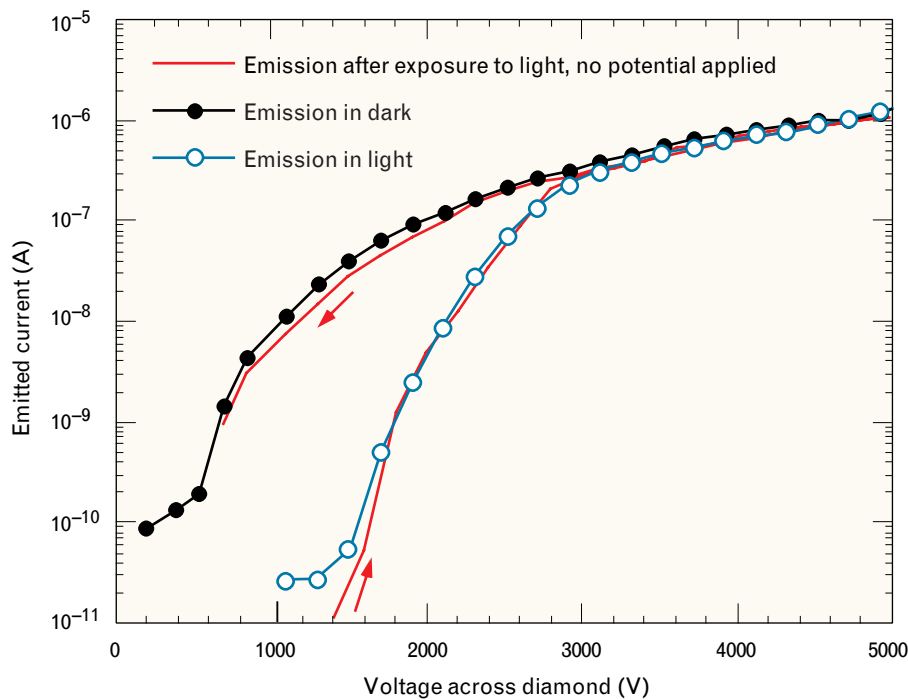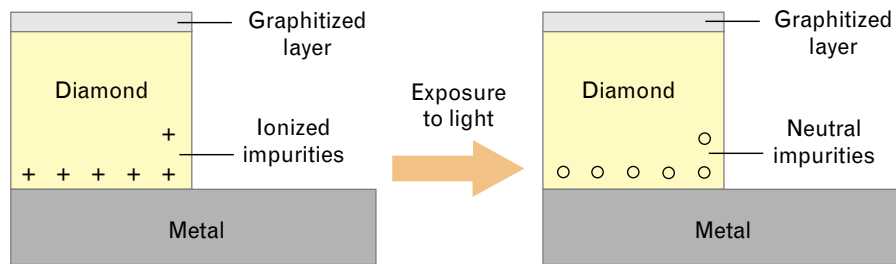
FIGURE 9. Emission current from diamond showing the effect of 100 W m^{-2} of incandescent illumination. (a) In the dark, emission occurs for potentials as low as 150 V. With the illumination on, emission is not measurable until the potential is greater than 1 kV. The red curve shows the emission after the cathode has been illuminated for one minute with no applied potential, and then a range of potentials are applied in the dark. (b) To explain the reduced electron emission caused by incandescent illumination, we believe the light neutralizes positive charges near the triple junction, which reduces the electric field at the triple junction and decreases the electron-tunneling current from the metal substrate.

the emission current exceeds about 10^{-7} A, the emission changes and the characteristics of the emitted current are nearly identical with emission in the dark (black curve).

We theorize that when the diamond is illuminated at low applied voltages, the dopants near the diamond surface are photoneutralized, so the electric field at the metal-diamond-vacuum triple junction is not suf-

ficient to cause emission. At voltages above 2.5 kV, significant emission occurs, which can reionize these dopants faster than they can be photoneutralized. At these larger voltages, sufficient electric field develops to enhance emission. Once the dopants are neutralized, emission even in the dark is poor until sufficient potential is applied across the diamond to reionize them.
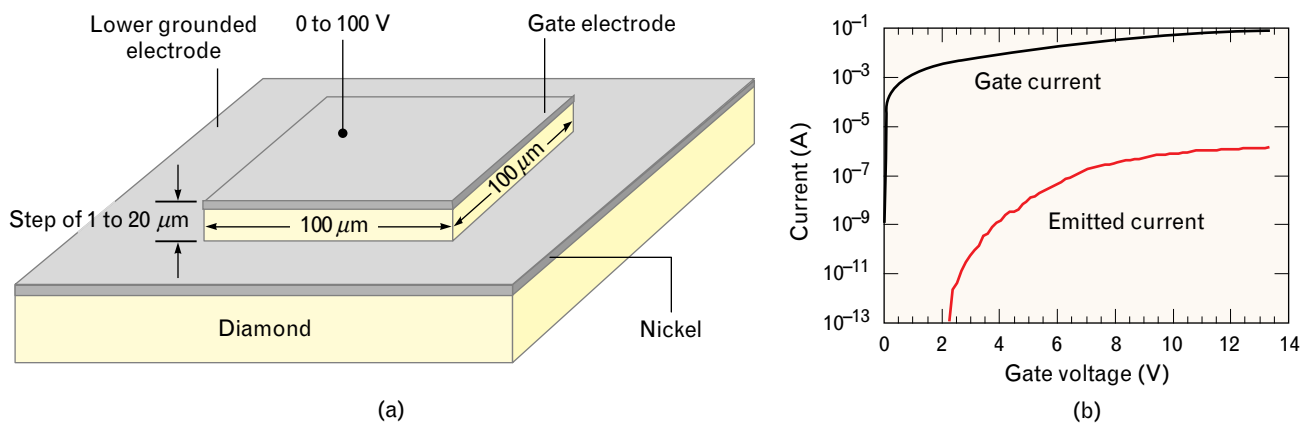
FIGURE 10. (a) Diagram of the cross section of a diamond surface-emission cathode consisting of type-Ib diamond in which 100×100-μm raised surfaces were formed by ion-beam-assisted etching. The gate and grounded electrodes consist of 50 nm of nickel. (b) Emitted current and gate current as a function of gate voltage for a diamond surface-emission device with a surface step height of 1.5 μm. Currents required for flat-panel displays—greater than 10^{-7} A—are obtained at gate voltages less than 10 V.

Practical Cathodes

We performed these experiments on comparatively thick diamond substrates. A more practical approach for low-voltage emission is to use ion-beam-assisted etching [28] to form surface structures in diamond, as shown in Figure 10. In this cathode, instead of the 100-μm surface length used in the previous experiments, a 1-to-20-μm surface step separates the nickel electrodes, and measurable emission occurs at a substantially lower voltage of 4 V, as shown in Figure 10(b). Emission from these surface devices is consistent with tunneling over a barrier. Figure 11 shows that the geometric electric-field enhancement mechanism and the Schottky-diode electric-field enhancement mechanism both result in similar predictions for the emitted current.

For devices with surface step heights less than 20 μm, the emission drops below the Fowler-Nordheim predictions of Equation 1 for electric fields (gate voltage divided by step height) above 20 V μm^{-1}. This drop may be caused by space charge or heating of the cathode from excessive gate current. At higher electric fields above 30 V μm^{-1} the cathode does not burn out, which happens with vacuum-field emission cathodes and diamond-grit-based cathodes [2, 6, 7]. Instead, the emission degrades and decreases with increasing gate voltage. When the cathode shown in Figure 10 is fabricated in thermally grown silicon di-

oxide on a silicon wafer, rather than in diamond, no measurable emission current is obtained even with gate voltages exceeding 100 V.

These diamond-based surface-emission cathodes operate reliably in poor vacuum environments and have been tested successfully in 1 Torr of nitrogen. Several devices on different substrates were fabricated over several months and the devices worked with consistent emission properties, unlike previous diamond-grit-based cathodes [2]. At present, the current to the top gate electrode is 10^2 to 10^5 times larger than the emitted current for the etched devices. We believe that this excess gate current can be reduced because we have been able to manufacture similar devices in which the emitted current exceeds the gate electrode current, as shown in Figure 7.

Non-Diamond Surface-Emission Cathodes

This section discusses non-diamond surface-emission cathodes as a background for the model used to explain diamond cathodes. K. Shoulders [29] observed that electrons appear to move on some insulating surfaces and that such a property might be useful for cathodes. G. Dittmer [30] and P.G. Borziak et al. [31] reported surface-emitting cathodes that operate by passing current through thin films made of metal islands that are 1 to 1000 nm in diameter on an insulating glass surface. A variety of film materials have been used for this type of surface-emitting cathode,
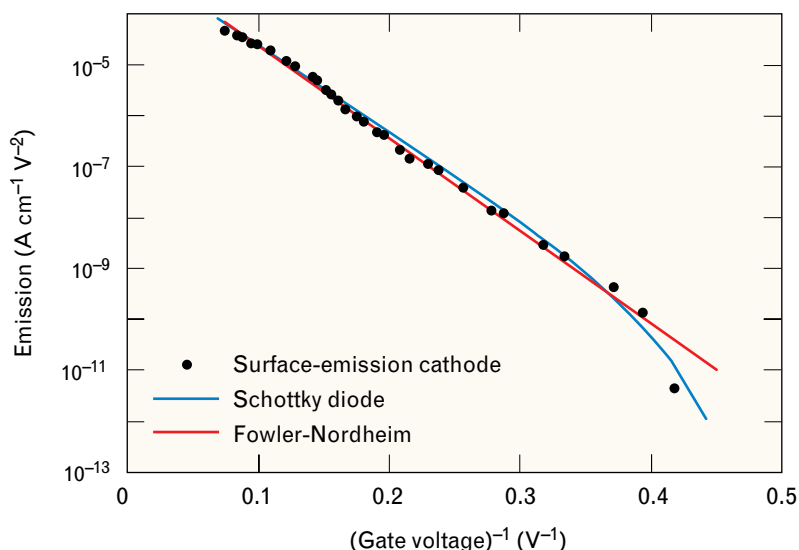
FIGURE 11. Emission-current data from the surface-emission cathode shown in Figure 10, plotted in Fowler-Nordheim coordinates over the voltage range of 3 to 11 V. The Fowler-Nordheim line represents a least-square fit to the data. The Schottky-diode emission curve was empirically fit to the data by using Equation 3 with $\Psi = 2.2$ eV and $J = 2.6 \times 10^{-3} P^{-2} \exp^{-40T}$.

including metals (cesiated gold), semimetals (carbon) [32], and semiconductors (indium tin oxide) [33, 34]. Recently, researchers at Canon have investigated palladium-oxide surface cathodes for use in flat-panel displays [35–37].

Non-diamond and diamond surface-emitting cathodes have much in common. Their geometries consist of metal electrodes separated by an insulating surface. Both cathodes exhibit the same electrical properties: (1) electrons are emitted with a narrow energy spread [30, 32, 37]; (2) emission increases with the addition of cesium or cesium salts [30]; (3) often a small fraction of the current flowing across the surface is emitted into vacuum; and (4) the emission current depends on the voltage across the cathode by the Fowler-Nordheim equation. The similarities between non-diamond and diamond cathodes suggest that both types of cathodes operate with the same emission mechanism. Three models for this emission mechanism have been proposed: (1) electron tunneling into vacuum at the enhanced electric field of the small (less than 10-nm-diameter) metal islands [30]; (2) thermal emission of hot electrons produced by electron conduction in the high electric fields between the metal islands [38]; and (3) scattering and

diffraction of energetic electrons out of the film by the metal islands [32].

Because the emission is related to the voltage across the film by the Fowler-Nordheim equation, Dittmer has argued that the emission mechanism is the result of electron tunneling. However, Y.A. Kulyupin discussed that the Fowler-Nordheim emission could also be the result of thermal emission [39]. R. Blessing et al. proposed that thermal and tunneling mechanisms both play a role in emission [40]. According to Blessing, thermal emission occurs primarily at voltages below 8 V, and electron tunneling dominates at higher voltages. A. Asai believes a large fraction of the electrons emitted into vacuum are pulled back to the cathode by the local electric fields, where they may be again elastically scattered back into vacuum [36]. He uses this model to explain the dependence of emission current on the anode voltage for his palladium-oxide cathodes. None of these models addresses the narrow energy spread of the emitted electrons. Voltages across the film vary from 6 to 50 V; if the entire film emits electrons, then the electron energy spread is expected to exceed the approximate number of 2 eV reported by several researchers [30, 32, 37]. Dittmer found that the size of metal islands for his films was smaller

near the negative electrode than in the rest of the film and suggested that the small energy spread results from emission occurring only from these small islands near the negative electrode.

The model we propose to explain diamond surface-emission cathodes—a triple junction composed of a doped semiconductor (diamond), metal, and vacuum—is an extension of the electron-tunneling model for surface-film cathodes. Field enhancement is primarily caused by the positive space charge in the semiconductor at the triple junction. As discussed by Asai, the electric field in the vacuum causes the electrons tunneling into the vacuum to fall onto the cathode surface. However, instead of relying on elastic scattering to reemit these electrons, we theorize that a barrier exists at the diamond-vacuum interface that prevents the electrons from entering the diamond. The electrons are then accelerated along the diamond surface away from the triple junction, gaining sufficient energy to be emitted into the vacuum.

Two other models might explain emission from the diamond cathodes. A surface discharge on the diamond could generate a plasma and hot electrons, which may be thermally emitted into the vacuum. The exceptionally high secondary electron yield of cesium-coated diamond [41, 42] could enhance electron secondary generation, making a surface discharge more likely to form. If the discharge is responsible for emission, then the energy spread of the emitted electrons will approach that of the potential applied across the diamond. As shown in Figure 8(b), the energy spread is orders of magnitude smaller than the applied potential. Alternatively, emission could occur not from the triple junction, but from some asperity on the negative electrode independent of the diamond substrate. In that case the incandescent light would not affect emission, contradicting the experimental data shown in Figure 9.

Conclusion

In the first publication that demonstrated low-field emission from diamond, M.E. Kordesch wrote, "The area between the crystallites (which are easily identified as depressions or crevices . . .) are strongly emitting areas" [43]. That is, the emission does not occur from the tips of the diamond facets by geometric electric-field enhancement, but from between the crystallites in the film where either the metal substrate or graphite layer separating the crystallites can serve as the conductive region of a triple junction. This observation suggests that many of the reported emission properties of diamond and diamond-like films result from the surface emission of triple junctions rather than from field emission from the bulk of the diamond into the vacuum. Kumar independently used the triple-junction model to explain diamond and diamond-like field emission [44].

We propose a new diamond electron-emission mechanism that relies on electric-field emission of electrons at a triple junction onto the NEA surface of diamond. Once on this surface, the electrons are accelerated to sufficient energies to be emitted into the vacuum. This electron-emission mechanism requires the diamond surface to intersect the conducting substrate at a triple junction.

The cathodes designed to maximize the new emission mechanism have more consistent emission than our previous grit-based cathodes [2]. They have some of the lowest reported operational voltages, they can emit a nearly monoenergetic, collimated beam of electrons with energies up to 6 keV, and they can operate in pressures of 1 Torr of nitrogen. This new emission mechanism also explains the previously reported reduction of emission with light [26]. In addition to diamond, several other materials such as organic salts formed with alkali metals and crown ethers [45], lithium fluoride [46], aluminum nitride [47], calcium fluoride [48], boron nitride [49], and cesium-doped glass surfaces may be useful for surface-emission cathodes.

Acknowledgments

REFERENCES

1. M.E. Kordesch, private communication.
2. M.W. Geis, J.C. Twichell, and T.M. Lyszczarz, "Fabrication and Theory of Diamond Emitters," *Linc. Lab. J.* **8** (2), 1995, pp. 161–171; M.W. Geis, J.C. Twichell, and T.M. Lyszczarz, "Diamond Emitters Fabrication and Theory," *J. Vac. Technol. B* **14** (3), 1996, pp. 2060–2067.
3. C.H. de Tourreil and K.D. Srivastava, "Mechanism of Surface Charging of High-Voltage Insulators in Vacuum," *IEEE Trans. Electr. Insul.* **8** (1), 1973, pp. 17–21.
4. R.V. Latham, "Appendix: Flashover across Solid Insulators in a Vacuum Environment," in *High Voltage Insulation: The Physical Basis* (Academic, London, 1981), pp. 229–240.
5. C.C. Grimes, "Electron in Surface States on Liquid Helium," *Surf. Sci.* **73** (1), 1978, pp. 379–395.
6. W.D. Dyke and W.W. Dolan, "Field Emission," in *Advances in Electronics and Electron Physics* **8**, L. Marton, ed. (Academic, New York, 1956), pp. 89–185.
7. C.A. Spindt, I. Brodie, L. Humphrey, and E.R. Westerberg, "Physical Properties of Thin-Film Field Emission Cathodes with Molybdenum Cones," *J. Appl. Phys.* **47** (12), 1976, pp. 5248–5263.
8. C.O. Bolzler, C.T. Harris, S. Rabe, D.D. Rathman, M.A. Hollis, and H.I. Smith, "Arrays of Gated Field-Emitter Cones Having 0.32 μm Tip-to-Tip Spacing," *J. Vac. Sci. Technol. B* **12** (2), 1994, pp. 629–632.
9. A.F. Myers, S.M. Camphausen, J.J. Cuomo, J.J. Hren, J. Liu, and J. Bruley, "Characterization of Amorphous Carbon Coated Silicon Field Emitters," *J. Vac. Sci. Technol. B* **14** (3), 1996, pp. 2024–2029.
10. E.I. Givargizov, V.V. Zhirnov, A.V. Kuznetsov, and P.S. Plekhanov, "Cold Emission from the Single-Crystalline Microparticle of Diamond on a Si Tip," *J. Vac Sci. Technol. B* **14** (3), 1996, pp. 2030–2033.
11. V.V. Zhirnov, G.J. Wojak, W.B. Choi, J.J. Cuomo, and J.J. Hren, "Wide Band Gap Materials for Field Emission Devices," to be published in *J. Vac. Sci. Technol. B.*
12. R.V. Latham, "Recent Advances in the Understanding of Prebreakdown Electron Emission," in *High Voltage Insulation: The Physical Basis* (Academic, London, 1981), pp. 211–227.
13. A. van der Zeil, *Solid State Physical Electronic* (Prentice-Hall, Englewood Cliffs, N.J., 1968), pp. 144–146.
14. P. Lerner, P.H. Cutler, and N.M. Miskovsky, "Theoretical Analysis of Field Emission from a Metal Diamond Cold Cathode Emitter," *J. Vac. Sci. Technol. B* **15** (2), 1997, pp. 337–342.
15. K. Okano, S. Koizumi, S.R.P. Silva, and G.A.J. Amaratunga, "Low-Threshold Cold Cathodes Made of Nitrogen-Doped Chemical-Vapour-Deposited Diamond," *Nature* **381**, 9 May 1996, pp. 140–141.
16. T.S. Sudarshan, J.D. Cross, and K.D. Srivastava, "Prebreakdown Processes Associated with Surface Flashover of Solid Insulators in Vacuum," *IEEE Trans. Electr. Insul.* **12** (3), 1977, pp. 200–208.
17. A. Watson, "Pulse Flashover in Vacuum," *J. Appl. Phys.* **38** (5), 1967, pp. 2019–2023.
18. M.W. Cole, "Properties of Image-Potential-Induced Surface States of Insulators," *Phys. Rev. B* **2** (10), 1970, pp. 4239–4252.
19. R.M. Osgood and X. Wang, "Image States on Single-Crystal Metal Surface," to be published in *Solid State Physics* (Academic, New York).
20. E.G. McRae, "Electronic Surface Resonances of Crystals," *Rev. Mod. Phys.* **51** (3), 1979, pp. 541–568.
21. C.C. Grimes and T.R. Brown, "Direct Spectroscopic Observation of Electrons in Image-Potential States outside Liquid Helium," *Phys. Rev. Lett.* **32** (6), 1974, pp. 280–283.
22. S. Prawer, C. Uzan-Spaguy, G. Braunstein, and R. Kalish, "Can *n*-type Doping of Diamond Be Achieved by Li or Na Ion Implantation?" *Appl. Phys Lett.* **63** (18), 1993, pp. 2502–2504.
23. S. Prawer and R. Kalish, "Ion-Beam-Induced Transformation of Diamond," *Phys. Rev. B* **51** (12), 1995, pp. 15 711–15 722.
24. M.W. Geis, J.C. Twichell, J. Macaulay, and K. Okano, "Electron Field Emission from Diamond and Other Carbon Materials after H_2, O_2 and Cs Treatment," *Appl. Phys. Lett.* **67** (9), 1995, pp. 1328–1330.
25. T.W. Mercer and P.E. Pehrsson, "Cs on Diamond," to be published.
26. M.W. Geis, J.C. Twichell, N.N. Efremow, K. Krohn, and T.M. Lyszczarz, "Comparison of Electric Field Emission from Nitrogen-Doped, Type Ib Diamond, and Boron-Doped Diamond," *Appl. Phys. Lett.* **68** (16), 1996, pp. 2294–2296.
27. H.-J. Fitting, G.O. Müller, R. Mach, G.U. Reinsperger, T. Hingst, and E. Schreiber, "Vacuum Emission of Hot Electrons from ZnS," *Phys. Stat. Sol. A* **121** (1), 1990, pp. 305–313.
28. N.N. Efremow, M.W. Geis, D.C. Flanders, G.A. Lincoln, and N.P. Economou, "Ion-Beam-Assisted Etching of Diamond," *J. Vac. Technol. B* **3** (1), 1985, pp. 416–418.
29. K. Shoulders, private communication.
30. G. Dittmer, "Electrical Conduction and Electron Emission of Discontinuous Thin Films," *Thin Solid Films* **9** (3), 1972, pp. 317–328.
31. P.G. Borziak, Y.A. Kulyupin, S.A. Nepijko, and V.G. Shamonya, "Electrical Conductivity and Electron Emission from Discontinuous Metal Films of Homogeneous Structure," *Thin Solid Films* **76** (4), 1981, pp. 359–378.
32. H. Araki and T. Hanawa, "The Temperature Dependence of Electron Emission from a Discontinuous Carbon Film Device between Silver Film Electrodes," *Thin Solid Films* **158** (12), 1988, pp. 207–216.
33. M.I. Elinson, A.G. Zhdan, G.A. Kudintseva, and M.E. Chugunova, "The Emission of Hot Electrons and the Field Emission of Electrons from Tin Oxide," *Radio Eng. Electron. Phys.* **10** (8), 1965, pp. 1290–1296.
34. M. Hartwell and C.G. Fonstad, "Strong Electron Emission from Patterned Tin-Indium Oxide Tin Films," *Int. Electron Devices Mtg.*, *Washington, 1–3 Dec. 1975,* pp. 519–521.
35. M. Yamanobe, Y. Osada, I. Nomura, H. Suzuki, T. Kaneko, H. Kawade, Y. Sato, Y. Kasanuki, T. Takeda, S. Mishina, N. Nakamura, H. Toshima, A. Isono, N. Suzuki, Y. Todokoro, and E. Tamaguchi, European Patent No. EP 0 605 881 A1, 28 Dec. 1993.
36. A. Asai, M. Okuda, S. Matsutani, K. Shinjo, N. Nakamura, K. Hatanaka, Y. Osada, and T. Nakagiri, "Multiple-Scattering Model of Surface-Conduction Electron Emitters," *Society for Information Display Int. Symp. Digest of Technical Papers* **28**, *Boston, 12–17 May 1997,* pp. 127–130.
37. E. Yamaguchi, K. Sakai, I. Nomura, T. Ono, M. Yamanobe, N. Abe, T. Hara, K. Hatanaka, Y. Osada, H. Yamamoto, and T. Nakagiri, "A 10-in. Surface-Conduction Electron-Emitter Display," *Society for Information Display Int. Symp. Digest of Technical Papers* **28**, *Boston, 12–17 May 1997,* pp. 52–55.
38. P. Borziak, Y. Kulyupin, and P. Tomchuk, "Electron Processes in Discontinuous Metal Films," *Thin Solid Films* **30** (1), 1975, pp. 47–53.
39. Y.A. Kulyupin and S.A. Nepiiko, "Effect of Substrate Deformation on Electron Emission from Dispersed Metal Films,"

Sov. Phys. Solid State **17** (9), 1975, pp. 1822–1824.

40. R. Blessing and H. Pagnia, "Electron Emission from Gold Island Films," *Phys. Stat. Sol. B* **110** (2), 1982, pp. 537–542.

41. G.T. Mearini, J.L. Krainsky, J.A. Dayton, Jr., Y. Wang, C.A. Zorman, J.C. Angus, and D.F. Anderson, "Stable Secondary Electron Emission from Chemical Vapor Deposited Diamond Films Coated with Alkali-Halides," *Appl. Phys. Lett.* **66** (2), 1995, pp. 242–244.

42. J.E. Yater, A. Shih, and R. Abrams, "Electron Transport and Emission Properties of C(100)," *Phys. Rev. B* **56** (8), 1997, pp. R4410–R4413.

43. C. Wang, A. Garcia, D.C. Ingram, M. Lake, and M.E. Kordesch, "Cold Field Emission from CVD Diamond Film Observed in Emission Electron Microscopy," *Electron. Lett.* **27** (16), 1991, pp. 1459–1460.

44. N. Kumar, "Diamond Cold Cathode Technology for FED Manufacturing," *DARPA High Definition Systems Information Exchange Conf. Proc., Arlington, Virg., 23–26 Mar. 1997.*

45. J.L. Dye, "Electrides: Ionic Salts with Electrons as the Anions," *Science* **247** (4943), 1990, pp. 663–668.

46. D.A. Lapiano-Smith, E.A. Eklund, F.J. Himpsel, and L.J. Teminello, "Epitaxy of LiF on Ge(100)," *Appl. Phys. Lett*. **59** (17), 1991, pp. 2174–2176.

47. M.C. Benjamin, C. Wang, R.F. Davis, and R.J. Nemanich, "Observation of a Negative Electron Affinity Heteroepitaxial AlN on a(6H)-SiC(0001)," *Appl. Phys. Lett.* **64** (24), 1994, pp. 3288–3290.

48. B. Quiniou, W. Schwarz, Z. Wu, R.M. Osgood, and Q. Yang, "Photoemission from Thick Overlying Epitaxial Layers of CaF_2 on Si(111), *Appl. Phys. Lett.* **60** (2), 1992, pp. 183–185.

49. M.J. Powers, M.C. Benjamin, L.M. Porter, R.J. Nemanich, R.F. Davis, J.J. Cuomo, G.L. Doll, and S.J. Harris, "Observation of a Negative Electron Affinity for Boron Nitride," *Appl. Phys. Lett.* **67** (26), 1995, pp. 3912–3914.
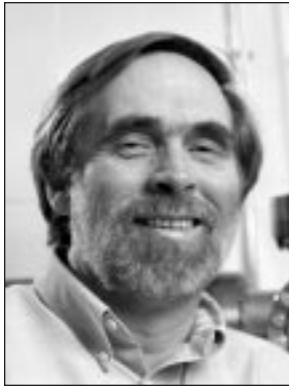
MICHAEL W. GEIS
is a staff member in the Submicrometer Technology group. His research interests are in diamond emitters and chemical sensors. He received a B.A. degree in physics, an M.S. degree in electrical engineering, and a Ph.D. degree in space physics and astronomy, all from Rice University. He has been at Lincoln Laboratory since 1978.

NIKOLAY N. EFREMOW, JR.
is an assistant staff member in the Submicrometer Technology group, where he fabricates and characterizes diamond emitters for flat-panel displays. After finishing his military service in the U.S. Navy in 1964, he joined Lincoln Laboratory to test high-power microwave components for radars. Later he helped set up and run the photolithographic laboratory, where he developed the conformable lithographic mask technology. He helped to construct a clean-room laboratory for submicrometer photolithography, producing state-of-the-art lithographic patterns with laser holography. He also worked on single-crystal diamond growth and ion-beam-assisted etching. Nikolay holds an associate degree in electrical engineering from Franklin Institute.

KEITH E. KROHN
oversees the operation of lithographic and etching tools in the fabrication laboratory of the Submicrometer Technology group. In his two decades at Lincoln Laboratory, Keith has contributed to research and fabrication in crystal growth, including graphoepitaxy, etching fine structures in diamond for traveling wave tubes, diamond transistors, and field emission cathodes. In addition, he has studied silicon recrystallization and device technology, and fabricated traveling wave structures, diamond transistors, and field-emission cathodes. Keith holds an associate degree in business science from Hesser Community College.

JONATHAN C. TWICHELL
is a staff member in the Submicrometer Technology group. His current research interests are in the electronic applications of diamond. Before joining Lincoln Laboratory in 1985, he worked at the University of Oklahoma. He received an A.B. degree in physics from Earlham College, and M.S. and Ph.D. degrees in nuclear engineering from the University of Wisconsin at Madison.

THEODORE M. LYSZCZARZ
is assistant leader of the Submicrometer Technology group. His background is in circuit design and integrated-circuit fabrication, with a special interest in scanning electron-beam lithography. His current research interests are in nanofabrication technology and applications. He received S.B., S.M., and Ph.D. degrees in electrical engineering from MIT.
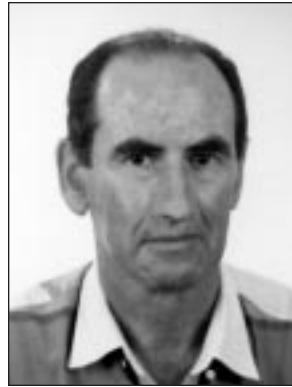
RAFAEL KALISH
is professor of physics and holds a chair in electronics at the Solid State Institute of the Technion-Israel Institute of Technology. His current research focuses on modifying the electronic properties of diamond, mainly by ion implantation. He received a M.Sc. degree in physics from Hebrew University and a Ph.D. degree in physics from the Weizmann Institute.

JAMES A. GREER
designs and sells laser deposition and ion-beam equipment for material deposition and modification for Epion Corporation in Bedford, Mass. He also researches extending pulsed-laser deposition and ion-beam processing to larger-area substrates. He graduated from Stevens Institute of Technology with a B.S. degree in mathematics, and M.S. and Ph.D. degrees in physics.

MARTIN Đ. TABAT
designs, builds, and tests pulsed-laser deposition equipment for Epion Corporation in Bedford, Mass. He previously worked for Raytheon Research Division in Lexington, Mass., developing pulsed-laser deposition processes. He graduated form California State University at Long Beach with a B.S. degree in physics.